Actuation and sensing for PZT micromirrors using d_{33} mode directional interdigitated electrodes

Pooja Thakkar, Anton Lagosh, Madeleine Petschnigg, Dominik Holzmann, Jaka Pribošek*

Silicon Austria Labs GmbH, Villach, Austria

*jaka.pribosek@silicon-austria.com

***Abstract*—This work explores the use of directional interdigitated electrodes leveraging d_{33} mode polarization for mode-selective actuation and sensing of micromirrors. To this end, a direct torsional actuation is achieved by 45° directional interdigitated electrodes and boosted by mechanical amplification. The torsion mode response is improved by 23% by poling the PZT layer in favor of the actuation mode. The d_{33} sensing scheme also proves to be 63x better than d_{31} sensing scheme for torsion mode response and 90x better for bending mode. The work demonstrates new flexibility in the design of next generation piezo MEMS actuators.**

Keywords—1D PZT micromirrors, PZT poling, Polarization, d_{33} mode, interdigitated electrodes, sensing.

I. INTRODUCTION

The d_{33} piezoelectric mode has primarily found its application in surface acoustic wave sensors and energy harvesting applications. This is mainly attributed to its increased piezoelectric coefficient and its capacity to create and harness in-plane stress distributions [1]. In contrast, the effective induction of significant out-of-plane actuation has been primarily accomplished through d_{31} mode excitation, which facilitates efficient direct bending action; consequently, the utilization of the d_{33} mode for substantial out-of-plane actuation has garnered relatively limited attention thus far. Comprehensive study on stress distribution, layout design for parallel plate electrodes and interdigitated electrodes (IDEs) was shown by [2], [3]. Among the reported work which employs this d_{33} mode for micromirrors, the applications are focused on quasistatic actuation [4]. For resonant micromirrors application, a deflection angle of 1.5° and a Q factor of 27 achieved at 10 V_{PP} and 6.1 kHz was reported by Grinberg et al. [5]. Kim et al. [6] worked on a micromirror array driven by IDEs cantilevers, showing static mirror deflection angles of ±8.9° at 85 V. The resonant frequency of this mirror is 400 kHz, but further investigations on dynamic performance in terms of scan angles and Q factor were not done. In our previous work, we reported 1D micromirrors actuated with d_{33} mode combined with mechanical amplification, achieving a state-of-the-art scan angle of 20° at 29.7 kHz and a Q factor of 2481 [7].

In this paper, we adapt the previous design using 45° IDEs optimized for torsion mode response, with a modified gap of 4 µm and electrode width of 7 µm, to accommodate batch fabrication process for different mirrors [8], [9]. The Si device layer thickness was also reduced from 175 µm to 150 µm to increase the scan angle and somewhat reduce the resonant frequency. We show that the performance of the directional IDEs can be improved by poling the PZT which allows to suppress the spurious d_{31} mode and improves its performance in both driving and sensing operation.

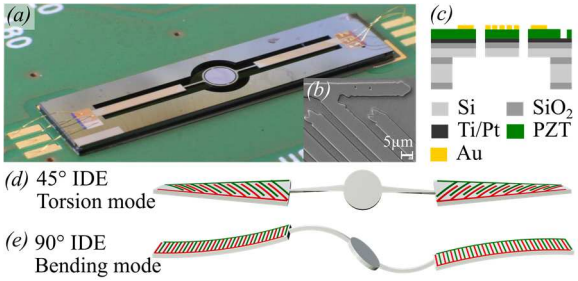

Fig. 1. (a) PZT Micromirror with IDEs on cantilever (b) Optical-SEM of IDEs (c) Fabricated device layer stack, Si 150 µm, SiO_2 2 µm, Ti/Pt 220 nm, PZT 1.7 µm, Au 220 nm (d) 45° IDEs micromirror in resonance (e) 90° IDEs micromirror in resonance (right cantilever actuated).

II. ACTUATION AND POLING OF PZT LAYER

A. Actuation and sensing mechanism

The d_{31} and d_{33} modes are analyzed in detail for actuation and sensing applications. In order to assess the performance of d_{33} mode actuation, we compare the mechanical response versus the one achieved by d_{31} mode actutaion of the same piezoelectric actuators (Fig. 2 (c), (b) respectively). For d_{31} actuation, which produces out-of-plane polarization, the two sets of IDE fingers (indicated in red F1 and green F2) are interconnected and supplied with both a common DC bias and an alternating voltage signal, Fig. 2 (a). Here, the bottom electrode is grounded.

The d_{33} actuation induces in-plane stress, but this can only be effectively achieved either by reducing the ratio between the finger gap and the thickness of the piezo layer or with a design without bottom electrode actuation [7]. In our current design, the bottom electrode enforces the equal electrostatic potential, which, due to the electrode geometry, gives rise to the significant and unwanted contribution of out-of-plane polarization, Thus, applying a positive and negative bias with 180° phase shifted signals on two sets of fingers Fig. 2 (a), results in both twisted and bent cantilever due to, both, in-plane and out-of-plane polarization. To mitigate this and reduce the spurious bending due to out-of-plane polarization, we poled the PZT in plane such that the domains between the fingers are aligned with the in-plane applied electric field used for actuation (Fig. 3 (c)). The strained membranes at torsion response can be sensed using two schemes. Firstly, d_{31} mode sensing aims to measure induced charges across the

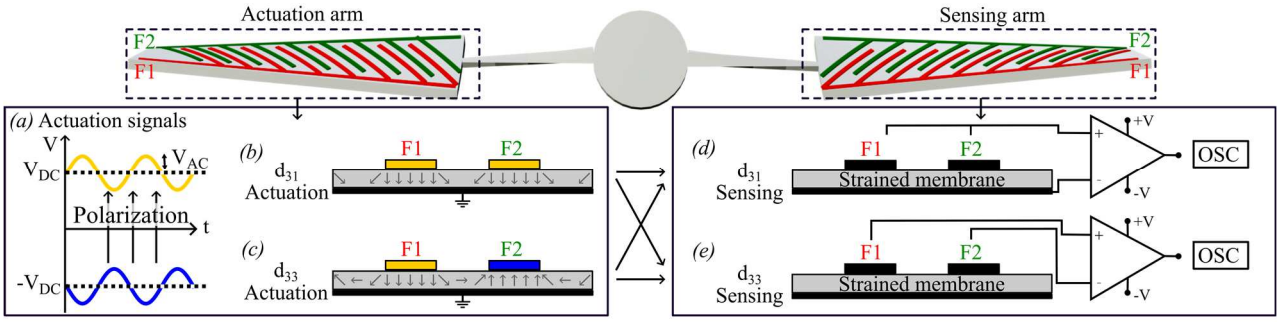

Fig. 2. Left arm is an actuation arm driven with signals (a), yellow and blue signals are 180° shifted to induce the in-plane stress. (b) and (c) demonstrate the unit cell cross-section of IDEs with d_{31} and d_{33} actuation scheme respectively. Right arm is a sensing arm where (d) and (e) are unit cells referring to sensing schemes for strained PZT layer. Arrows visualize all four possible combinations between different actuation and sensing modes.

layer, using the same idea of interconnecting the two IDEs finger sets and measuring its signal differentially with bottom electrode (Fig. 2 (d)). Secondly, the d_{33} mode sensing aims to measure induced charges between the fingers (Fig. 2 (e)).

B. *PZT poling method*

The PZT was poled favoring the d_{33} mode (Fig. 3 (a)) using an aixACCT TF2000 piezo analyzer. First, the temperature was increased to 150°C, then an electric field of 6.25 MV/m was applied with a rise time of 30 s, followed by a hold time of 900 s. The temperature was gradually lowered to room temperature and the bias was removed. P-E (Polarization-Electric field) hysteresis loops were measured before and after the poling, which shows a built-in field of 3.3 V. Fig. 3 (b) and (c) show the unpoled sample and a sample with residual polarization in the PZT layer respectively. This will enhance the d_{33} mode actuation while d_{31} actuation will get suppressed as the residual orientation of domains around IDEs opposes the externally applied electric field (Fig. 3 (d), (e)).

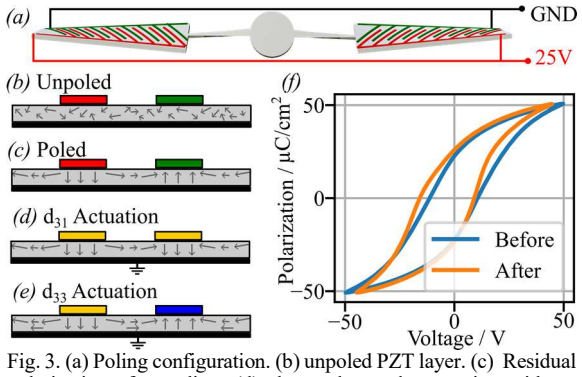

Fig. 3. (a) Poling configuration. (b) unpoled PZT layer. (c) Residual polarization after poling. (d) shows d_{31} mode actuation with an applied external field on poled sample. (e) improved d_{33} mode actuation when an external electric field is applied on poled sample. (f) P-E hysteresis loop before and after the poling treatment.

III. EXPERIMENTAL RESULTS

A. *Experimental setup*

A custom experimental setup was built to allow us measuring the frequency response, optical phase delay of micromirrors and test various sensing schemes. Driving electronics comprise of a signal generator 33500B series from Keysight and a homebuilt amplifier OPA541 for actuation. The torsional and bending response of the micromirror is measured optically using a position-sensitive device (PSD) 718-DL100-7-PCBA3 (First Sensor, Berlin, Germany) enabling the precise measurements of optical scan angles (OSA) and optical phase delay with respect to driving signals. A low-power instrumentation amplifier AD8421 used in differential amplifier configuration with a gain of 10 is employed for sensing. All signals are recorded with a digital oscilloscope PicoScope 4824a for post-processing.

B. *Effect of poling and d_{33} mode performance*

Prior to poling, the mirrors frequency response (Fig. 4 (b), (d) plots with blue markers), shows that the torsion response due to d_{33} actuation is higher than d_{31} actuation by 1.5° at 10 V_{PP}. This is attributed to additionally induced in-plane polarization due to d_{33} actuation on the top of out-of-plane polarization. The same measurement was repeated after poling (Fig. 4 (b), (d) plots with red markers) and an amplitude increase from 7.3° to 9° at 10 V_{PP} was obtained for the d_{33} actuation (23% relative increase). Consequently, a torsional response obtained for d_{31} actuation was found to reduce upon poling from 5.8° to 4.6° (21%). This is anticipated, as residual polarization opposes the externally applied field. Contrarily to torsion mode response from two actuation schemes, the bending mode response due to d_{33} actuation is lower than d_{31} actuation. As the poled 45° IDEs are optimized for torsion mode, the energy dissipation increases while in bending mode operation. In addition, the springs can be further optimized to improve the performance of bending mode, which was not intended here.

C. *Frequency response tests*

After poling the sample, we perform frequency response test for 45° IDEs (Fig. 4 (a)-(d) plots with red markers). The torsion mode response is higher than bending mode response for both d_{31} and d_{33} actuation schemes, demonstrating the selectivity for 45° rotated IDEs. For d_{33} actuation, the torsion mode response is four times better than the bending mode. This can be attributed to the following three contributions: (i) the induced in-plane stress in the direction perpendicular to the 45° IDEs (ii) the residual polarization resulting from PZT poling, and the last (iii) the in-plane stress in the direction parallel to the IDEs. This combined effect results in a large torsional response as seen in Fig. 4 (b), (d). For d_{31} actuation, the torsional response is two times better than bending response (yet lower as compared to d_{33} mode

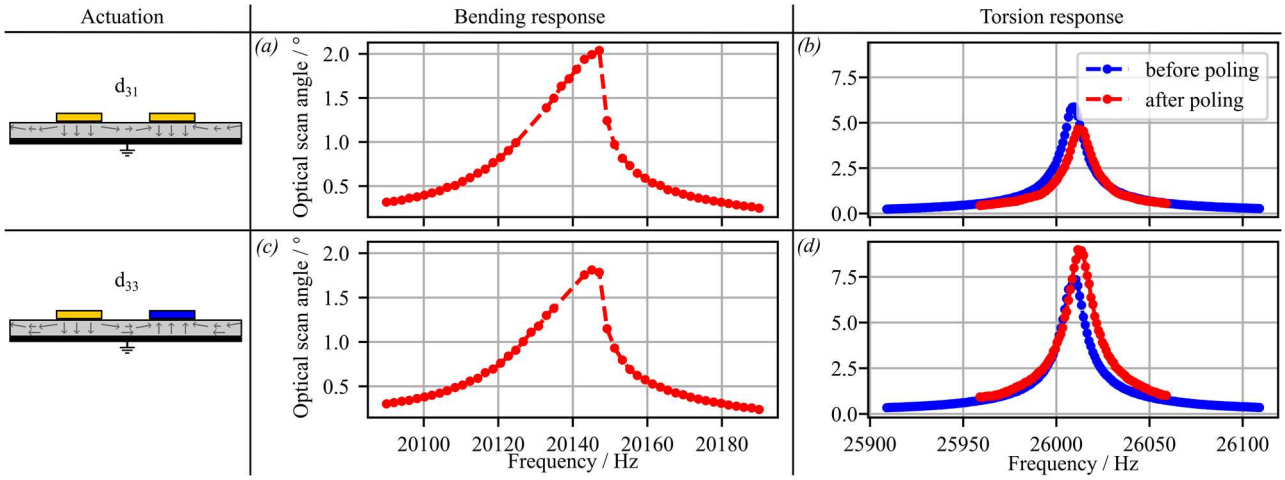

Fig. 4. Bending and Torsion response of 45° IDEs from d_{31} and d_{33} actuation at $10V_{PP}$. Please note the change in vertical scale between the bending and torsion response.

actuation), due to stiffening and opposing residual polarization.

D. Sensing tests

Next, we actuated one side of the mirror using the more efficient d_{33} mode (as in Fig.4 (c) and (d)), while the other side of the mirror (as in Fig.2) was used for sensing. The d_{31} and d_{33} sensing response were measured and compared. The scan angle of 1.8° for bending mode response of micromirror results in sensing signals of 182 mV for d_{33} sensing scheme and 2 mV for d_{31} sensing scheme (Fig. 5 (a)). For torsion mode response at the scan angle of 9.0°, 760 mV of the d_{33} sensing signal and 12 mV of d_{31} sensing signal are measured (Fig. 5 (b)). The d_{33} sensing proves to be more than 90 times better than the d_{31} sensing for bending mode, and 63 times for torsion mode. Sensitivity of 10 mV/° for bending mode response and 8.4 mV/° for torsion mode response is reached with respect to d_{33} sensing mechanism. As a contrast, d_{31} sensing mechanism has a much lower sensitivity of 0.16 mV/° for torsion mode. While for bending mode, the signal is at the noise level, rendering it not useful as a feedback signal.

Next, we measured the phase delay between the driving signal and sensing signal of the d_{33} mode and compared it to the delay obtained with the reference optical signal, as measured with the PSD. A phase delay difference of 7.6°±0.2° between sensing and optical response was obtained throughout the entire frequency range, with rather constant phase around the resonant frequency. Sensing signals thus show large potential to be used for optical angle tracking. In future, IDEs design will be explored for different combinations of 45° and 90° IDEs, together with favorable poling of PZT. Further investigation on improvement for sensing and actuation for dedicated modes is required.

IV. Conclusion

Poling of the PZT layer for dedicated torsion response mode, which uses d_{33} mode, results in increased torsion response by 23% and thus improved the d_{33} sensitivity as well. The d_{33} sensing using 45° IDEs proves to be superior to d_{31} sensing, where a large d_{33} sensing signal of 750 mV was measured for torsion mode at 9° OSA after poling. These results show the potential for new design freedom that d_{33} mode can offer for next generation piezo MEMS devices.

Acknowledgment

Authors would like to thank TDK Electronics GmbH & Co OG, Deutschlandsberg, Austria for development and fabrication of PZT thin films. The chips were fabricated at SAL MicroFab, Silicon Austria Labs GmbH, Villach, Austria. We would like to thank Takashi Sasaki, Silicon Austria Labs GmbH, for the assistance with the mask layout.

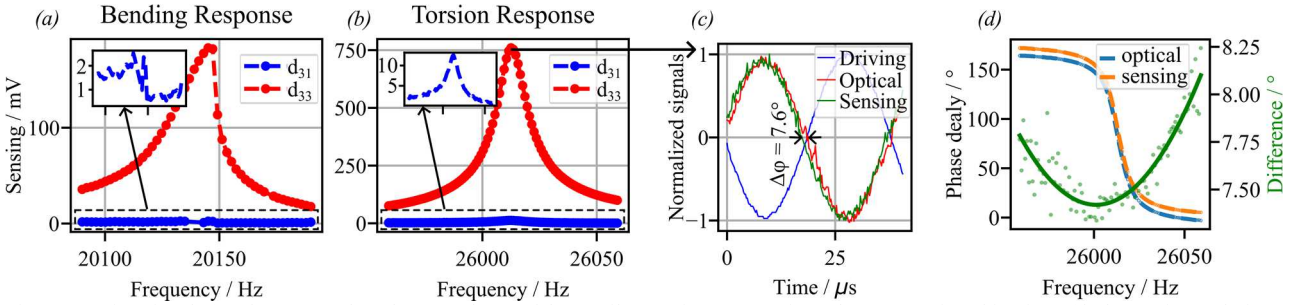

Fig. 5. Sensing signals (a), (b) measured on the second arm of the cantilever using two sensing schemes mentioned in Fig. 2 (d) d_{31} sensing and Fig. 2 (e) d_{33} sensing, and for the actuation scheme as in Fig. 4. (c), (d) respectively. (c) Snapshot of driving, optical response, and d_{33} sensing signals measured at resonance for d_{33} actuation and torsional response at $10V_{PP}$. (d) Optical and sensing phase delay signals, their difference (in green) for d_{33} actuation and torsional response.

REFERENCES

[1] S. Priya *et al.*, "A Review on Piezoelectric Energy Harvesting: Materials, Methods, and Circuits," *Energy Harvesting and Systems*, vol. 4, no. 1, pp. 3–39, Jan. 2017, doi: 10.1515/ehs-2016-0028.

[2] M. C. Wapler, M. Stürmer, J. Brunne, and U. Wallrabe, "Piezo films with adjustable anisotropic strain for bending actuators with tunable bending profiles," *Smart Mater. Struct.*, vol. 23, no. 5, p. 055006, May 2014, doi: 10.1088/0964-1726/23/5/055006.

[3] A. Mazzalai, "PZT thin films for MEMS devices: from in-situ sputter deposition to energy harvesting device," EPFL, Lausanne, 2014. doi: 10.5075/epfl-thesis-6375.

[4] I. (Hotzen) Grinberg, N. Maccabi, A. Kassie, S. Shmulevich, and D. Elata, "Direct Torsion of Bulk PZT Using Directional Interdigitated Electrodes," *Procedia Engineering*, vol. 168, pp. 1483–1487, 2016, doi: 10.1016/j.proeng.2016.11.429.

[5] I. Grinberg, N. Maccabi, and D. Elata, "A pure-twisting piezoelectric actuator for tilting micromirror applications," in *2017 19th International Conference on Solid-State Sensors, Actuators and Microsystems (TRANSDUCERS)*, Kaohsiung, Taiwan: IEEE, Jun. 2017, pp. 2035–2038. doi: 10.1109/TRANSDUCERS.2017.7994472.

[6] D.-H. Kim, J.-W. Jeon, K. S. Lim, and J.-B. Yoon, "Development of 16μm×16μm Digital Micromirror Array Suitable for Seamless-picture Projection Display System".

[7] P. Thakkar, A. Lagosh, T. Sasaki, M. Bainschab, and J. Pribošek, "Resonant d33 Mode PZT Mems Mirror Excited with Directional Interdigitated Electrodes," in *2023 IEEE 36th International Conference on Micro Electro Mechanical Systems (MEMS)*, Jan. 2023, pp. 1127–1130. doi: 10.1109/MEMS49605.2023.10052304.

[8] J. Pribošek, A. Lagosh, P. Thakkar, T. Sasaki, and M. Bainschab, "Resonant Piezoelectric Varifocal Mirror with on-Chip Integrated Diffractive Optics for Increased Frequency Response," in *2023 IEEE 36th International Conference on Micro Electro Mechanical Systems (MEMS)*, Jan. 2023, pp. 1131–1134. doi: 10.1109/MEMS49605.2023.10052247.

[9] A. Lagosh *et al.*, "Novel Piezoelectric MOEMS Platform: Micro and Nano Engineering (MNE) and EUROSENSORS 2022," 2022. Accessed: Jun. 15, 2023. [Online]. Available: https://www.mne2022.org/images/Detailed_Programme_-_FINAL_LS.pdf